Colloids and Surfaces B: Biointerfaces 107 (2013) 160–166

Contents lists available at SciVerse ScienceDirect

Colloids and Surfaces B: Biointerfaces

journal homepage: www.elsevier.com/locate/colsurfb

Lipid-based microtubes for topical delivery of Amphotericin B

Claudia Salerno[a,*], Diego A Chiappetta[a,b], Alicia Arechavala[c], Susana Gorzalczany[d], Silvia L Scioscia[a], Carlos Bregni[a]

[a] Department of Pharmaceutical Technology, Faculty of Pharmacy and Biochemistry, University of Buenos Aires. Buenos Aires, Argentina
[b] National Science Research Council (CONICET), Argentina
[c] Mycology Unit. Hospital de Infecciosas F. J. Muñiz. CABA. Argentina
[d] Department of Pharmacology, Faculty of Pharmacy and Biochemistry, University of Buenos Aires. Buenos Aires, Argentina

ARTICLE INFO

Article history:
Received 2 November 2012
Accepted 4 February 2013
Available online 13 February 2013

Keywords:
Lipid microtubes
Self-assembly
Amphotericin B
Topical delivery

ABSTRACT

The self-assembly process is a valuable tool for constructing nano and microstructures. Microtubes (MTs) self-assembled from amphiphiles are novel promising nanomaterials as they have easy self-assembly in aqueous solutions, reproducibility and biocompatibility. The incorporation of amphotericin B (AmB) into lipid microtubes formed from 12-hydroxystearic acid (12HSA) when mixed with ethanolamine in aqueous media was investigated. MTs of several concentrations of lipid material and AmB were prepared. The structure was characterized by phase-contrast microscopy, TEM and SEM. The type of interaction was analyzed by FTIR and DSC. Stability studies were carried out at room temperature and at 4 °C. Loading efficiency of the system was found to be much higher than the drug solubility in water. MTs with 1% of 12HSA and 1 mg/ml of AmB showed to be the most stable formulation. In vitro skin penetration assay showed a flux of $18.20 \pm 3.35\ \mu g/cm^2$. Amb-loaded MTs in vitro antifungal activity was evaluated and formulation showed similar results to that of AmB deoxycholate showing that AmB retained its antifungal activity in the MTs formulation.

1. Introduction

Since the discovery of carbon nanotubes there have been reports on a variety of tubular micro and nanostructures. The self-assembly process is a valuable tool for obtaining different types of these structures and plays an important role in the discovery of novel nanomaterials with application in regenerative medicine and drug delivery systems. Self-assembled organic tubular structures are hollow tubes that have advantages like easy fabrication process at low temperature and low cost. Three-dimensional structures are formed from molecular association through intermolecular forces such as van der Waals forces, electrostatic interactions, hydrogen bonding, and various π–π stacking interactions [1,2].

Lipid tubes consist of bilayers packed concentrically. A limited number of natural and synthetic lipids can assembly into tubular structures such as glycolipids, bola form derivatives and phospholipids; tube-forming lipids are in general chiral molecules which also form helically coiled ribbons [3,4].

Amphiphilic molecules can self-assembly into various morphologies (micelles, rods, tubes and vesicular aggregates) depending on initial conditions of concentration, pH and temperature. These supramolecular assemblies including tubes, helices, twisted ribbons and cochleate cylindres have collectively been called complex high axial ratio microstructures (CHARMs). Testosterone incorporation into CHARMs has been studied by Goldstein et al. (2001) [2,5].

Lipid-based microtubular structures have been investigated as drug delivery systems used to provide slow and sustained release for several proteins such as Transforming Growth Factor- β, myoglobin and thyroglobulin and some drugs as tetracyclines and 2-methoxy naphthalene. Also, bone morphogenetic proteins were incorporated into lipid tubes to overcome short half-life [6,7], and Henricus et al. (2008) examined the interactions of insulin with MTs formed from a bola-amphiphile as potential delivery system to prevent aggregation of the protein [8].

A growing focus is being set on the use of microtubes and nanotubes because of their large relative internal volume which can be functionalized, besides micro and nanomaterials would allow for more accurate intracellular and intercellular targeting. Microtubes (MTs) self-assembled from amphiphiles are promising biomaterials because they have easy self-assembly in aqueous solutions, reproducibility and biocompatibility.

Douliez et al. (2006) introduced MTs from 12-Hydroxystearic acid (12HSA) when mixed with ethanolamine (ETA) in aqueous media and later Novales et al. (2008) reported ethanolamine salts of 12HSA to form turbid birefringent lamellar dispersions.

* Corresponding author at: Junin 956. 6th floor – (1113). Buenos Aires, Argentina. Tel.: +54 11 49648271; fax: +54 11 49648271.
E-mail addresses: salernoclaudia@hotmail.com, salernoclaudia3@gmail.com (C. Salerno).

0927-7765/$ – see front matter © 2013 Elsevier B.V. All rights reserved.
http://dx.doi.org/10.1016/j.colsurfb.2013.02.001

Subsequently, Fameau et al. (2010) studied the formation of 12HSA MTs under various experimental conditions [4,9,10]. For MTs made of 12HSA and ETA as the counterion a previous chemical synthesis step is not required, in contrast to other lipid-forming tubes, which is an advantage if considered as potentially useful drug carriers. They are also simple to produce and there is no need for hazardous organic solvents.

Amphotericin B (AmB) is a polyene macrolid antifungal used for invasive infections caused by *Candida spp.* and *Aspergillus spp*., and also is a second line drug for the treatment of clinical diseases causes by the parasite *Leishmania spp*. AmB has a very low solubility in water (1 μg/ml) at physiological pH. In order to overcome this problem several strategies have been attempted such as liposomes, cochleates, lipid complexes and nanospheres; some of them have improved the therapeutic index of the drug and reduce adverse effects but they require higher doses and they are also very expensive [11,12].

MTs of 12HSA are formed in alkaline media and taking into account that AmB shows better water solubility in basic solutions we considered that it would be an advantage for loading the drug into these MTs. The aim of this work was to investigate the incorporation of AmB into MTs prepared from 12HSA, characterize the structure and evaluate stability. Also, in vitro skin penetration and in vitro antifungal activity of AmB-loaded MTs were tested in order to determine the potential of MTs as drug delivery system for topical use.

2. Materials and methods

2.1. Materials

12-Hydroxystearic acid (12HSA) was a gift from CASTOROIL S.A.C.I.A.F., Argentina; monoethanolamine (ETA) was a purchased from Sigma–Aldrich; Amphotericin B (AmB) Alpharma, was kindly supplied by Unifarma SA, Argentina; Carboxymethyl cellulose (CMC) was purchased from Fabriquimica S.R.L.; Amphotericin B Deoxycholate Northia®, Argentina; all other reagents were of pharmaceutical or analytical grade.

2.2. Microtubes preparation

Microtubes (MTs) were prepared using the method reported by Fameau et al. [10]. Briefly, the corresponding weight of 12HSA was placed in a glass vial and distilled water was added so that the final concentration was 0.5, 1 and 2, 5 and 7.5% w/v (0.5-MT, 1-MT, 2-MT, 5-MT, and 7.5-MT). Then, the appropriate volume of a 1 M stock solution of ETA was added to get 1:1 12HSA:ETA molar ratio. The mixture was heated at 75–80 °C in a water bath for 15 min until melting of the lipid, and then vigorously vortexed. MTs formed upon cooling of the clear isotropic solution. The yield of MTs was calculated from a known dilution of MTs (1/1000) counted on a hemocytometer, the observation was made at 10X (UNION MIC-3, Tokyo).

AmB-loaded MTs were prepared by adding the drug after heating the mixtures 12HSA/ETA, before the formation of MTs. Then, the systems were vortexed obtaining loaded-MTs with 1, 3, 5 and 7.5 mg/ml of AmB.

2.3. AmB loading and stability

AmB-loaded 1-MT dispersions were stored at room temperature and at 4 °C. The drug content was determined at fixed times. An aliquot of the MTs dispersions was filtered by 1.2 μm (GL Microfiber, Titan 2) and dissolved in methanol and drug concentration was determined by UV spectrophotometry (UV–vis Spectrophotometer Shimadzu UV-260) at 406 nm, using a calibration curve of AmB in methanol covering the range 0.5–10 μg/ml (correlation factor 0.9995–1.000) using methanol as blank. Assays were done in triplicate.

In order to determine drug loading into MTs, AmB in ETA aqueous solutions (in the same concentration as used for MTs preparation) were prepared and filtered by 0.45 μm nylon filter (MC Microsolv) and 1.2 μm (GL Microfiber, Titan 2). AmB was determined in both filtrates, and compared with the filtrates of AmB-loaded MTs dispersions through the same filter size. Also, AmB solubility in distilled water and in 12HSA was determined. Assays were made in triplicate.

2.4. Phase-contrast microscopy

Phase-contrast microscopy was used to confirm the formation of MTs, evaluate whether the inclusion of AmB showed any change in structure morphology and to evaluate length of MTs. Microscopy observations were made at 20× and 40× magnification using an Axioskop 2 Plus, Zeiss, Germany, equipped with a Sony Exwave HAD video camera to collect digital images (768 × 494 pixels). A drop of the MTs dispersion was placed on the glass-slide and covered with a cover slip without any treatment. The glass-slides were previously cleaned with ethanol and acetone.

2.5. Scanning electron microscopy (SEM)

1-MT dispersions both loaded and unloaded were lyophilized and analyzed by SEM. Sample was affixed to carbon tape on a specimen stub and excess powder removed. The stubs were stored under vacuum overnight. The samples were sputter-coated with gold. Electron micrographs were obtained using a Field Emission Gun Scanning Electron Microscope (FEG-SEM Zeiss Supra™ 40 apparatus Gemini column, Germany) operating at 1.0 kV accelerating voltage.

2.6. Transmission electron microscopy (TEM)

1-MT dispersions both loaded and unloaded were analyzed by TEM using a transmission electron microscope Zeiss 10C with Kodak 5302 photographic film. Samples were prepared as follows:after shaking the MTs dispersions a drop was placed on a copper grid with a Formvar membrane for 30 s, then excess liquid was removed using a piece of filter paper. The grid was covered with a drop of uranyl acetate 2% aqueous solution for 30 s and excess liquid was removed using a piece of filter paper.

2.7. Thermal analysis

Differential scanning calorimetry (DSC, Mettler Toledo TA-400 Differential Scanning Calorimeter, Columbus, OH, USA) was used to evaluate interactions between AmB and lipid material. AmB raw active compound, 12HSA and lyophilized 1-MT loaded and unloaded were analyzed. Samples (4–9 mg) were sealed in 40 μl Al-crucible pans and heated from 25 to 250 °C under nitrogen atmosphere. DSC curves were recorded at constant heating rate of 10 °C/min.

2.8. FT-IR spectroscopy

FT-IR spectra of AmB and 12HSA as received, and MTs dispersions both loaded and unloaded were recorded on a Nicolet 380 FT-IR Spectrometer with ATR (attenuated total reflectance) cell (ZnSe) for liquids (12 reflexions) using Nicolet Omnic software. Samples were dispersed in hexane and the dispersions were placed on the crystal plate for liquids and allow the solvent to evaporate

before obtaining the measurements. The patterns were recorded between 400 and 4000 cm^{-1}.

2.9. Zeta potential determination

Determination of zeta potential was carried out at 25 °C using a NanoZetasizer-ZS (Malvern Instrument, Malvern, UK). Zeta Potential was determined on diluted 1/100 samples to adjust within the operational limits of the instrument. The reported values are the average of at least 3 measurements.

2.10. In vitro skin penetration

In vitro skin penetration and permeation experiments were performed on Franz diffusion cells using pig ear skin. Pig ears were obtained from a local pork slaughterhouse for human feeding. However, approval has been obtained from the Ethical Committee for the Care and Use of Laboratory Animals of the Faculty of Pharmacy and Biochemistry, University of Buenos Aires (N° 170511-2). Skin was excised from 4-month-old domestic pig ears. Pig ears were cleaned under running water immediately after excision. The hair from the outer region of the ears was removed and then the skin was carefully separated from cartilage using a scalpel. Subsequently, adipose subcutaneous tissue was removed; Full-thickness skin was used with a surface area of 3.14 cm^2. Thickness of 1 mm for all the samples was controlled with a vernier. After being dried with a tissue, the skin was immediately mounted on the diffusion cells or frozen at −20 °C for a maximum period of 4 weeks [13].

The skin was placed horizontally on Franz diffusion cells, between the donor and receptor compartments. Sink conditions were obtained in the receptor compartment with phosphate-buffered saline (PBS; pH 7.4) with 1% sodium lauryl sulfate (PBS-LSNa; pH 7.4). The volume of receptor fluid was 15 ml. The receptor compartment was continuously homogenized using a stirring magnetic bar and the temperature was kept at 32 °C using a water circulation system.

The skin mounted in the cell was allowed to rest for an hour in contact with receptor media before the application of the samples. AmB-loaded 1-MT (1 mg/ml) thickened with CMC 2% was assayed and compared with a hydrogel prepared from AmB Deoxycholate (marketed formulation) reconstituted with distilled water, according to instructions, and thickened with CMC 2%. Experiments were performed applying 200 μg of AmB as dose.

Serial sampling (6 ml) was performed after 0.5, 1, 2, 4 and 6 h. Fresh PBS-LSNa was added to receptor compartment in order to replace the receptor medium. Aliquots were filtered by 0.45 μm nylon filter (CAMEO) and analyzed by HPLC (Shimadzu SPD-10 A vp Uv/Vis Detector). A Microbore C18 (150 × 2.0 mm, 3 μm) Waters Spherisorb® S3 ODS2 column was used with an isocratic mobile phase composed of acetonitrile:disodium edetate 2,5 mM (45:55) [14]. The injection volume was 20 μl and the flow rate was 0.4 ml/min, UV detection was set at 382 nm. Retention time was 4.0 ± 0.1 and 3.4 ± 0.0 min for samples in methanol and PBS-LSNa, respectively. Linearity curve was determined for the range 0.06–1.60 μg/ml (r^2 = 0.9989). External standard was also used during the measurements.

After the experiment (6 h), the remnant of the dosage form on the skin (*dislodgeable dose*) was put in a glass vial, skin was washed twice with methanol; the used spatula was also washed so as to collect the dosage form completely. The final volume was adjusted with methanol and the mixture was stirred (2500 rpm) for 1 h. The solution was filtered and AmB was quantified by HPLC as mentioned above. Skin drug penetration, considered as the amount retained within the skin, was calculated by difference between the total dose applied and the sum of the amount that permeated plus the amount present in the remnant sample over the skin.

2.11. In vitro antifungal activity

AmB-loaded 1-MT dispersions and AmB-loaded 1-MT thickened with CMC 2% were tested. The MIC (minimal inhibitory concentration) was determined according to M27-A3 CLSI method [15]. A suspension of *Candida* (1 × 10^6 UFC/ml) was incubated with 100 μl of solutions with different concentrations of the antifungal in DMSO (32–0.06 μg/ml) or the corresponding dilutions of the tested formulation in a 96-well plate at 35 °C for 48 h. Visual readings were performed after 24 and 48 h. The MIC was defined as the lowest drug concentration inhibiting clearly visible growth of the fungi. 100 μl of RPMI-solvent without AmB were placed in a well for growth control and 200 μl of RPMI-solvent in another well for sterility control. ATCC *C. parapsilosis* 22019 and *C. krusei* 6258 were used as control strains. AmB Deoxycholate from market (Anfotericina B Northia®, Argentina) was assayed as reference. AmB standard (used as reference in the Mycology lab) and AmB raw material (used for the MTs formulations) were tested as controls as well. Blank 1-MT was tested as negative control.

2.12. Skin irritation test

The backs of six albino rabbits (Gilardoni-Cabañas, Argentina) were clipped free of hair. AmB-loaded 1-MT (1 mg/ml) thickened with CMC 2% was tested on two one inch square sites on the same animal; one site was intact and one was abraded in such a way that the stratum corneum was opened but without bleeding. Formulations were tested undiluted (0.5 g). Each test site was covered with two layers of one inch square surgical gauze secured in place with tape. The entire trunk of the animal was then wrapped with rubberized cloth in order to retard evaporation and hold the patches in one position. Twenty-four hours after application, the wrappings were removed and the test sites evaluated for erythema and oedema. Evaluations of abraded and intact sites were separately recorded. Test sites were evaluated again 48 and 72 h after application by the same procedure. Maximal score was set in 8 [16]. Experiments involving animals were made according to international ethics and Approval has been obtained from the Ethical Committee for the Care and Use of Laboratory Animals of the Faculty of Pharmacy and Biochemistry, University of Buenos Aires (Exp-FyB 00747495/2012).

2.13. Statistical analysis

Data were analyzed using software MS Excel 2007 Data Analysis Add-In programme. *T*-Student's *t*-test was performed to see any significant difference ($p < 0.05$).

3. Results and discussion

3.1. Microtubes preparation

MTs of various 12HSA concentrations were prepared: 0.5, 1, 2, 5, and 7.5% (0.5-MT, 1-MT, 2-MT, 5-MT, and 7.5-MT). Lipid MTs were successfully produced using the self-assembly method previously described [10]. The formation of randomly oriented MTs was observed by phase-contrast microscopy (Fig. 1). According to Fameau et al., tubes are formed by periodically stacked bilayers, with water in the lamellar spacing. Reproducible formation implies that the tubular structures have a definite composition [10].

The length of the 1-MT measured by phase-contrast microscopy was in the range of 4.5–12.5 μm; TEM images confirmed an average size to be 8.5 μm and 0.7 μm for length and outer diameter,

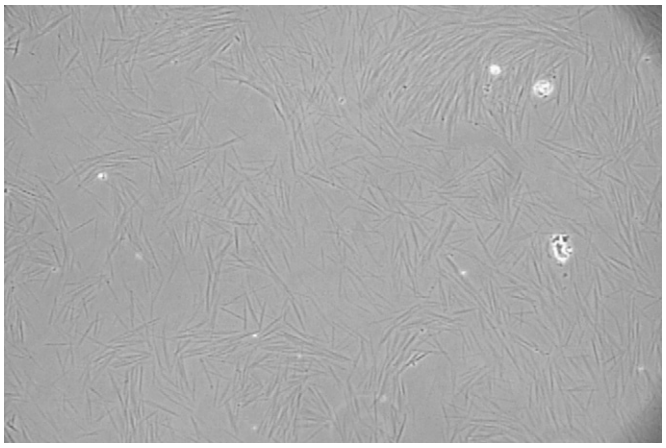

Fig. 1. Phase-contrast image of blank 1-MTs (40×).

respectively. TEM and SEM images (Fig. 2a and b) showed that MTs are twisted tubular structures. The yield of MTs for 1-MT was 4.11×10^8 MTs/ml. The dispersions appeared as white suspensions that separate after a few days of storage with a loose and easily redispersible sediment.

MTs of similar size were observed in 0.5-MT and 2-MT dispersions, but in 2-MT more MTs could be clearly observed. The aspect of these dispersions was similar to the 1-MT and also separate when stored.

In 5-MT and 7.5-MT dispersions a great deal of MTs were formed, some of them twice the size of the MTs seen in less concentrated systems, but also aggregates (*images not shown*). These more concentrated MTs systems appeared more viscous upon cooling and they did not flow from the vial so they were not further investigated for drug loading in this work.

AmB-loaded dispersions were prepared with 0.5-MT, 1-MT and 2-MT. AmB incorporation was favoured by the pH of the MTs dispersions (10.01 ± 0.10) because the drug is more soluble in basic solutions. All the concentrations 1, 3, 5 and 7.5 mg/ml could be incorporated in selected MTs dispersions. However, sediment was observed in 0.5-MT after one week and 2-MT showed a more pearly aspect with agglomerates; 2-MT dispersions with 3, 5 and 7.5 mg/ml of AmB also appeared darker. AmB loaded 1-MT systems with 1 and 3 mg/ml of AmB were stable dispersions without sediment or visual change during the study.

Phase-contrast microscopy images of loaded 1-MT with AmB 1 mg/ml and 3 mg/ml showed no alteration in aspect or size of the MTs when the drug was incorporated. Also, TEM and SEM images (Fig. 2c and d) showed no change in the inner part or in morphology of the MTs, suggesting that the drug would be part of the MT wall. On the contrary, 1-MT with 5 and 7.5 mg/ml of AmB showed the formation of vesicles and aggregates in addition to the MTs (*not shown*).

It was interesting to note that AmB-loaded 1-MT dispersions also separated when stored, except for the case of the one with 5 mg/ml of the drug; this was further analyzed by Z potential of the systems (see below).

3.2. AmB loading and stability

AmB solubility in 12HSA was very low as expected (0.62 ± 0.09 μg/ml and 5.09 ± 0.29 μg/ml was determined in 0.45 and 1.2 μm filtrates, respectively). AmB recovery in 1.2 μm ETA solutions filtrates and MTs dispersions filtrates was nearly the same. But when these samples were filtered by 0.45 μm AmB could filter from ETA solutions and recovered almost completely in the filtrate unlike the case of MTs in which the drug was withheld on the filter with the MTs (Table 1). Also, we could see by SEM and phase-contrast microscopy that aspect of raw drug and of

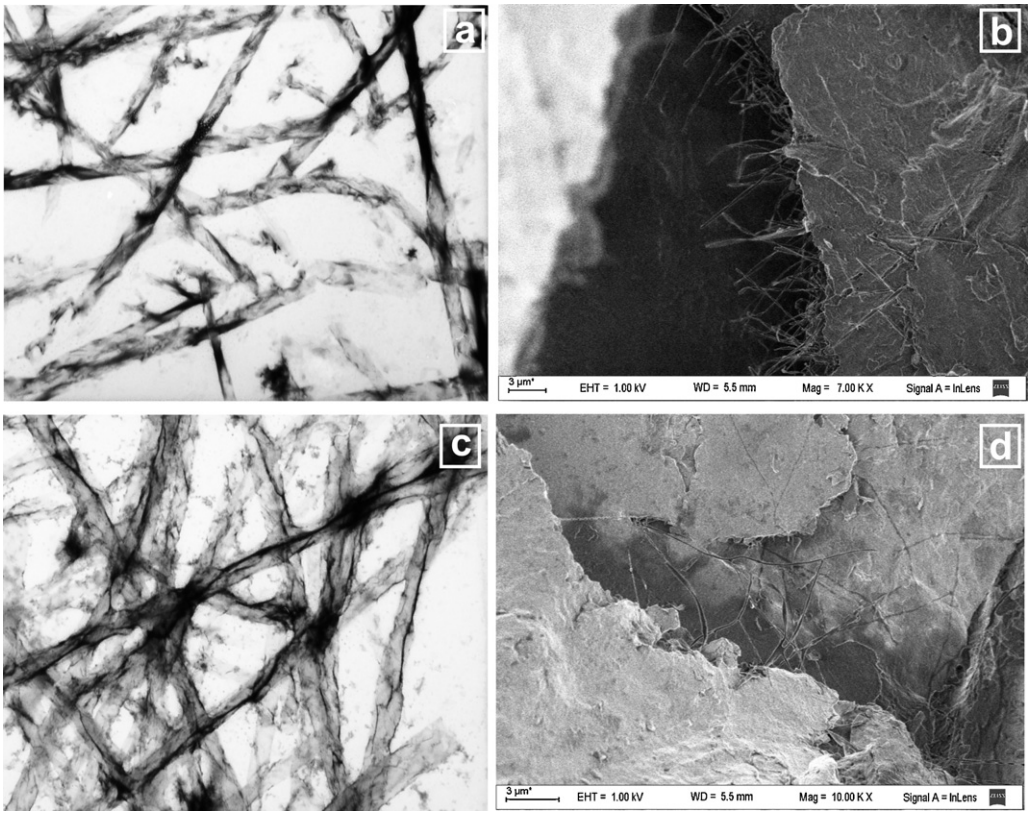

Fig. 2. TEM (3000×) (a) and SEM (b) images of blank 1-MT; TEM (3000×) (c) and SEM (d) images of 1-MT loaded with amphotericin B 1 mg/ml.

Table 1
Amphotericin B content in filtrates.

Sample	AmB concentration in 1.2 μm filtrate (μg/ml) (±SD)	AmB concentration in 0.45 μm filtrate (μg/ml) (±SD)	% entrapped in MTs
Distilled water	17.2 (4.0)	–	–
12HSA	5.1 (0.3)	0.6 (0.1)	–
AmB 1 mg/ml in ETA	1200.0 (8.0)	780.0 (100.0)	–
AmB 3 mg/ml in ETA	2760.0 (140.0)	2150.0 (300.0)	–
AmB 5 mg/ml in ETA	4600.0 (290.0)	4140.0 (80.0)	–
AmB- loaded 1-MT 1 mg/ml	1010.0 (10.0)	242.8 (1.3)	75.7
AmB- loaded 1-MT 3 mg/ml	2850.0 (150.0)	300.5 (0.1)	90.0
AmB- loaded 1-MT 5 mg/ml	4630.0 (110.0)	782.7 (2.1)	84.4

ETA solution filtrate were quite different from the corresponding images of MTs-AmB dispersions. This confirmed the presumption that the drug was incorporated into MTs.

AmB- loaded 1-MT stability is shown in Fig. 3. Dispersions with AmB 1 mg/ml were the most stable during the study both at room temperature and at 4 °C. AmB-loaded 1-MT dispersion remained stable for almost three months (T_{90} = 80.77 days) when stored at 4 °C.

3.3. Thermal analysis

3.3.1. Formation of microtubes

Thermal analysis (Fig. 4a) showed an endothermic peak at 78.11 °C (ΔH = −156.73 J/g) for raw 12HSA, according to literature, while the endothermic peak for the lyophilized 1-MT prepared with 1% of 12HSA was at 77.04 °C (ΔH = −140.98 J/g), which indicates the presence of a different entity.

3.3.2. AmB-loaded MTs

Several changes in endothermic peaks were observed for the AmB-loaded 1-MT (Fig. 4b). Peaks changed as follows: 77.04–69.69 °C for the lipid material and 140.28–118.18 °C and 194.92–161.55 °C for the endothermic peaks of AmB. In view of these results we investigated the behaviour of a physical mixture of lyophilized MTs and AmB raw material and in that case the enthalpogram showed no significant shift of the peaks, therefore we concluded that there was an interaction of the drug with 12HSA in the formation of MT wall, which was confirmed by the FT-IR spectra (see below).

3.4. FT-IR

In order to elucidate the driving forces involved in the self-assembly of the MTs and the loading of the drug, FT-IR analyses were performed.

3.5. MT formation

In Fig. 5a 12HSA spectrum shows peaks assignable to carboxylic acid at 1699.9 cm^{-1} for C=O stretching, several peaks at 1220–1298 for C—O stretching and a band at 3000–3350 for O—H stretching

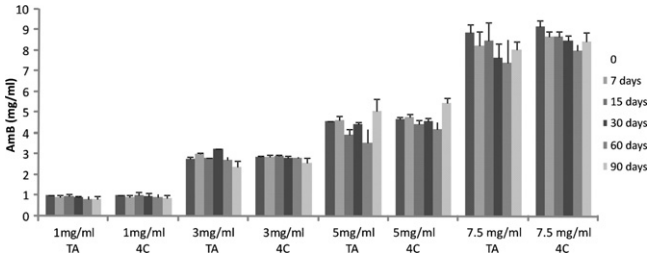

Fig. 3. Drug stability in 1-MT dispersions at 4 °C and 25 °C.

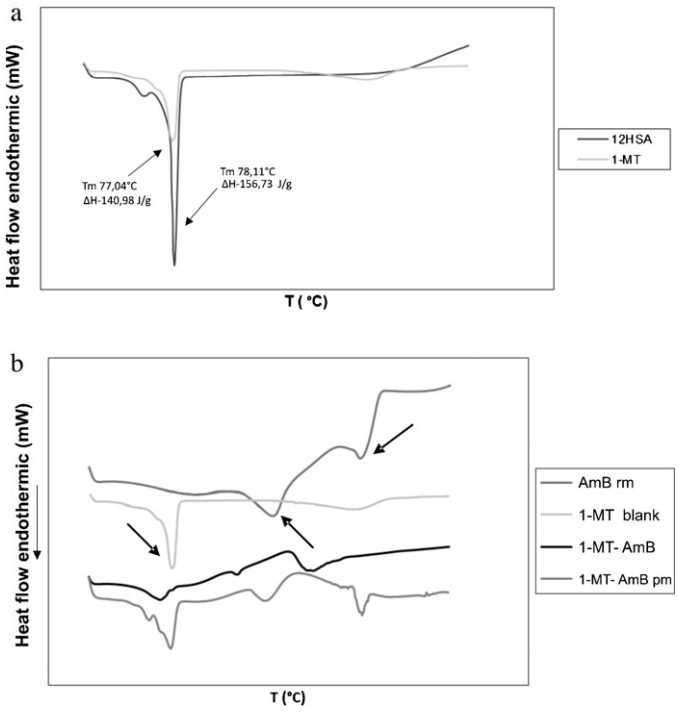

Fig. 4. Thermal analysis. a: Microtubes blank; b: microtubes loaded with amphotericin B (AmB) rm: drug as received; pm: physical mixture.

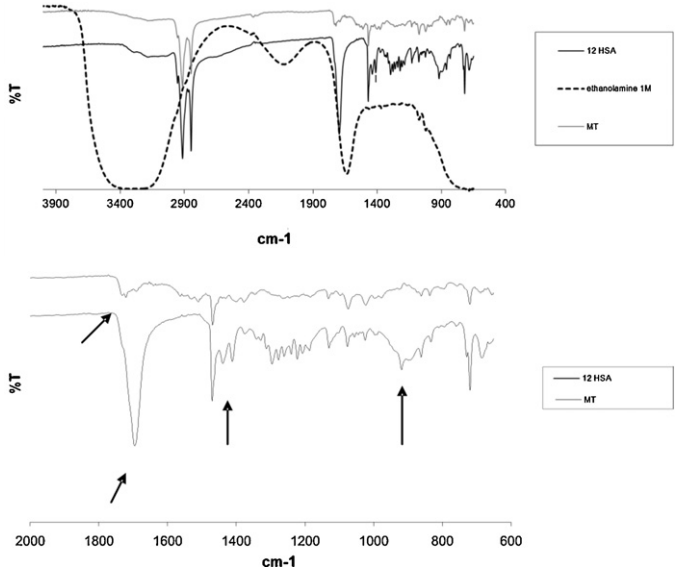

Fig. 5. FTIR spectra. 12HSA: 12 hydroxystearic acid; MT: microtubes.

vibration. Peaks corresponding to aliphatic alcohol are 3430 for O—H (H-bonded); 1414, 1439 and 1384 for O—H bending in plane; 687 for O—H bending out of plane and 920 for C—O stretch. For the alkyl chain: 2920, 2850 for CH_3—CH_2 alkane stretch, 1469.7 for CH_3— CH_2 bend, 1348.8 for CH_3 deformation, and the presence of CH_2 rocking at 720.3 cm^{-1} indicating a long-chain compound [17,18].

In the spectrum for 1-MT the decrease in carboxylic acid transmittance peak at 1700 cm^{-1} indicates that the acid has converted to a different functional group, which is confirmed by the appearance of a peak at 1737 cm^{-1} assignable to a C=O ester. There are also changes in peaks 1298 and 1220 for C—O in carboxylic acid. Changes observed for the transmittance peaks of the aliphatic alcohol are the absence of 1414, 1440 and 687.6 peaks for bending and the peak at 920 cm^{-1} for C—O stretching; also the broad band at 3000–3350 cm^{-1} attributable to O—H hydrogen bonded appears less intense. Probably the intermolecular H bond formation causes a decrease in the intensity of transmittance for the free OH [19].

Peak at 1639 cm^{-1} for primary N—H was not observed in 1-MT spectrum, which may also be involved in intermolecular association for the supramolecular assembly of the MTs.

3.6. AmB-loaded 1-MT

Fig. 6a shows the spectrum of AmB as received. The main peaks reported in literature are present (668 OH bending out of plane; 764.6 and 795 pyranose ring breathing; 835 band due to —CH_3, COO^- and NH_2 bending out of plane; 1008 and 1041 bending in plane for cromophore and —CH in transpolyene out of plane bending; 1067 bending out of plane NH_2, C—O—C pyranose ring; 1067,1132 and 1163 C=O asymmetric stretch (COC, COH); 1186 COC=O asymmetric stretch (β glycosidic linkage); 1401 —CH in plane bend polyene; 1556 polyene C=C stretch; 1690 symmetric stretching for COO^- [20–23].

The spectrum of AmB-loaded 1-MT showed no relevant difference in the region 3600–3000 cm^{-1} corresponding to intermolecular and intramolecular hydrogen bonding, supporting the idea that AmB is not loaded in the MTs by this type of interactions and also that the drug is not self- aggregated. This last inference is also backed up by the lack of signal at 1533 cm^{-1}, related to drug association in dimers, which is advantageous since adverse effects are related to the aggregated state of the drug [21].

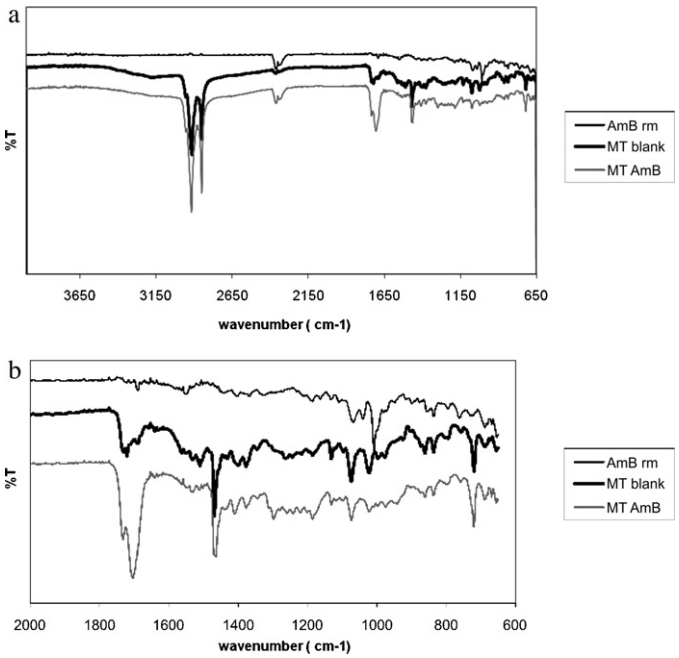

Fig. 6. FTIR spectra MTs loaded with amphotericin B (AmB). rm: Drug as received b: fingerprint area.

In the extended graph for the "finger print" area (2000–600 cm^{-1}; Fig. 6b) several important differences are identified. Peak at 1007 cm^{-1} corresponding to bending in plane for chromophores and —CH in transpolyene out of plane bending is of less intensity. Possibly π–π stacking interactions are favoured by the assembly which modifies this peak.

Peak at 1044 assigned to bend out of plane of —NH_2 and symmetric stretching C—O—C of pyranose ring by Gagóz et al. (2011) does not appeared [23]. Also, peak at 1072 for asymmetric stretching of C—O—C linking mycosamine moiety to the macrolactone ring of AmB is not observed. This changes could be interpreted in terms of the relative rotational freedom of the mycosamine moiety around C19—O42 and O42—C43 bonds which might be restricted owing to steric hindrance, electrostatic coupling or hydrogen bonding formation [21,22].

It is also evident that peak at 1722 present in blank MT, is not present for the case of AmB-loaded MT. Moreover, a new peak appeared at 1298 cm^{-1} and there is a noticeable difference in the broadened and intense peak at the frequency 1707 cm^{-1} compared to the peaks in blank MT at 1695 and AmB at 1693 as both these peaks are much smaller.

These results and the changes in DSC pattern allowed us to conclude that the loading of AmB molecules within the MTs resulted in drug-material interaction not only by hydrogen bonds.

3.7. Zeta potential

Zeta potential of both blank and loaded 1-MT dispersions was negative: −44.68 mV for blank 1-MT and −44.30, −45.77 and −40.73 mV for loaded dispersions with AmB 1, 3 and 7.5 mg/ml, respectively. AmB-loaded 1-MT with AmB 5 mg/ml was the one with the greater negative zeta potential, −51.13 mV, which could explain the observation that dispersions separated after a few days of store, except for the case of dispersions with 5 mg/ml of AmB which did not separated during the study.

No important changes were observed in the Z potential upon encapsulation, which indicate that the drug was encapsulated in the MTs and not absorbed on the outside as well, as the drug is negatively charged at basic pH [8].

3.8. In vitro skin penetration

Assay showed that penetration into pig ear skin was 28.63 ± 3.94% of applied dose (18.20 ± 3.35 μg/cm^2), with a flux of 3.05 ± 0.05 μg/cm^2/h during the assay with no permeation to receptor fluid. AmB deoxycholate sample revealed 99.65 ± 0.04% penetration of the applied dose, but drug was detected in receptor media after 1 h. The size of MTs could be one of the reasons of the lower penetration because carriers greater than 5 μm are not expected to go through stratum corneum. Also, the acidic pH of skin (4.2–5.6) could have caused the MTs to alter. Moreover, it was reported that the acidic pH of skin caused the aggregation of carboxylated polystyrene nanoparticles, as electrostatic forces would decrease at that pH condition, and aggregates would be less likely to penetrate the skin [24,25]. However, although drug delivery from MTs was low these results showed an improvement compared to reports on AmB skin penetration when a liposomes formulation was tested [15].

3.9. Skin irritation test

No irritation was observed on skin of the rabbits, the score was 0.42. No dermal lesions were observed at any time and the observed

Table 2
Amphotericin B (AmB) minimal inhibitory concentration (MIC) against different cultures. AmB D: Amphotericin B deoxycholate; rm: raw material; st: standard; CMC: carboxymethylcellulose.

Specie	Origin	MIC (μg/ml)				
		AmB D	AmB-loaded 1-MT	AmB-loaded 1-MT with CMC	AmB st	AmB rm
C. albicans	64548	0.030	0.060	0.060	0.250	0.060
C. albicans	549	0.030	0.060	0.125	0.125	0.060
C. albicans	40139	0.030	0.125	0.250	0.125	0.125
C. albicans	129	0.030	0.125	0.125	0.125	0.060
C. albicans	Hemoculture	0.030	0.060	0.060	0.125	0.060
C. albicans	Vaginal discharge	0.030	0.060	0.125	0.125	0.060
C. albicans	sputum	0.030	0.125	0.125	0.125	0.060
C. albicans	Oral mucosa	0.030	0.125	0.250	0.250	0.125
C. glabrata	Vaginal discharge	0.030	0.125	0.250	0.125	0.125
C. tropicalis	BAL	0.060	0.500	0.500	0.500	0.250
C. tropicalis	Hand nail	0.060	0.250	0.500	0.500	0.250
C. neoformans	Hemoculture	0.030	0.060	0.060	0.060	0.030
C. parapsilosis	ATCC 22019	0.030	0.250	0.250	0.125	0.125
C. krusei	ATCC 6258	0.030	0.250	0.250	0.250	0.500

slight erythema was reversible so the formulation is suitable for topical treatment.

3.10. In vitro antifungal activity

MIC of AmB-loaded 1-MT was determined for several strains of *Candida* and different patient isolates. AmB-loaded 1-MT dispersion was effective in the same extent as AmB deoxycholate for several samples. In some cases, MIC value for MTs formulation was slightly greater than market formulation in (Table 2). Also the thickened samples showed higher MIC in some cases. It is to consider that MIC values equal or less than 0.120 μg/ml are within assay variability and also that in same cases MIC value for controls (AmB standard and AmB raw material) was also greater than for AmB deoxycholate. However, MIC was lower than the one considered for resistant cultures (>2 μg/ml) in all the cases assayed. Blank formulations had no activity.

4. Conclusions

The present study reports the incorporation of AmB into lipid microtubes. AmB was successfully loaded into microtubes of 12HSA at concentration several times higher than drug solubility in water. Results indicate that AmB is interacting with the lipid material within the MT wall, which is consistent with the amphiphilic nature of the drug. AmB penetrated the stratum corneum and was retained within skin and it was shown that AmB retained its antifungal activity in the loaded MTs. AmB-loaded 1-MT may potentially be used as a delivery system for topical use. Further investigations should be made to study stability of lyophilized system in order to have a longer shelf life.

Acknowledgements

This work was financially supported with funds from Project UBACyT B003 (2008–2010) from University of Buenos Aires. Authors thank PhD Rafael Ricco for his support in the obtention of phase-contrast images and Prof. PhD Viviana CampoDall'Orto for her assistance in the obtention of FTIR spectra.

References

[1] H.Y. Lee, S.R. Nam, J.-I. Hong, J. Am. Chem. Soc. 129 (2007) 1040.
[2] M. Menzenski, I.A. Banerjee, New J. Chem. 31 (2007) 1674.
[3] H.Y. Lee, S.R. Nam, J.-I Hong, Chem. Asian J. 4 (2009) 226.
[4] J.-P. Douliez, C. Gaillard, L. Navailles, F. Nallet, Langmuir 22 (7) (2006) 2942.
[5] A.S. Goldstein, J.K. Amory, S.M. Martin, C. Vernon, A. Matsumoto, P. Yager, Bioorg. Med. Chem. 9 (2001) 2819.
[6] N.J. Meilander, X. Yu, N.P. Ziats, R.V. Bellamkonda, J. Control Release 71 (2001) 141.
[7] M.R. Johnson, H.-J. Lee, R.V. Bellamkonda, R.E. Guldberg, Acta Biomater. 5 (2009) 23.
[8] M.M. Henricus, K.T. Johnson, I.A. Banerjee, Bioconjugate Chem. 19 (2008) 2394.
[9] B. Novales, L. Navailles, M. Axelos, F. Nallet, J.-P. Douliez, Langmuir 24 (1) (2008) 62.
[10] A.-L. Fameau, B. Houinsou-Houssou, B. Novales, L. Navailles, F. Nallet, J.-P. Douliez, J. Colloid Interface Sci. 341 (2010) 38.
[11] A. Lemke, A.F. Kiderlen, O. Kayser, Appl. Microbiol. Biotechnol. 68 (2005) 151.
[12] N. Lincopani, E.M. Mamizukal, A.M. Carmona-Ribeiro, J. Antimicrob. Chemother. 52 (2003) 412.
[13] European Comission SCIENTIFIC COMMITTEE ON CONSUMER PRODUCTS (SCCP) Opinion on BASIC CRITERIA FOR THE IN VITRO ASSESSMENT OF DERMAL ABSORPTION OF COSMETIC INGREDIENTS - updated March 2006 http://ec.europa.eu/health/ph_risk/committees/04_sccp/docs/sccp_s_03.pdf
[14] A. Manosroi, L. Kongkaneramit, J. Manosroi, Int. J. Pharm. 270 (2004) 279.
[15] National Committee For Clinical Laboratory Standards (2002). Reference method for broth dilution antifungal susceptibility testing of yeasts. Approved standard M27-A2, 2nd ed. National Committee for Clinical Laboratory Standards, Wayne, Pa.
[16] J. Draize, G. Woodard, H. Calvery, J. Pharmacol. Exp. Ther. 82 (1944) 377.
[17] R. Awang, A.N. Azizan, S. Ahmad, W.M.Z.W. Yunus, J. Oil Palm Res. 19 (2007) 350.
[18] J. Coates, Encyclopedia of analytical chemistry, in: R.A. Meyers (Ed.), Interpretation of Infrared Spectra, A Practical Approach, John Wiley & Sons Ltd., Chichester, 2000, pp. 10815–10837.
[19] M.A. Varfolomeev, D.I. Abaidullina, A.Z. Gainutdinova, B.N. Solomonov, Spectrochimica Acta Part A: Molecular and Biomolecular Spectroscopy. 77 (5) (2010) 965.
[20] I.M. Asher, in: Florey Klaus (Ed.), Analytical Profiles of Drug Substances, vol. 6, Academic Press, New Jersey, 1977, pp. 1–42.
[21] M. Gagóz, G. Czernel, D.M. Kaminski, K. Kostro, Biometals 24 (5) (2011) 915.
[22] M. Gagóz, M. Arczewska, Biochim. Biophys. Acta 1798 (2010) 2124.
[23] M. Gagóz, M. Arczewska, J. Phys. Chem. B. 115 (2011) 3185.
[24] B. Baroli, J. Pharm. Sci. 99 (1) (2010) 21.
[25] T.W. Prow, J.E. Grice, L.L. Lin, R. Faye, M. Butler, W. Becker, E.M.T. Wurm, C. Yoong, T.A. Robertson, H.P. Soyer, M.S. Roberts, Adv. Drug Deliv. Rev. 63 (2011) 470.